Impact of Magnetic Focusing on the Origin of Electron Beams Propagating Upwardly in the Solar Corona

Bofeng Tang, Haihong Che, Gary P. Zank, and Vladimir Kolobov
Department of Space Science
The University of Alabama in Huntsville, Huntsville, AL, 35805, USA

Introduction

Solar type III radio bursts, first discovered by Wild & McCready (1950), are believed to be produced by electron beams via an electron two-stream instability (ETSI). Recently discovered radio bursts showed that electrons beams are commonly produced in solar flares. Numerous nanoflare-associated radio bursts were discovered, implying that electron beams are distributed widely in the solar corona and very probably contribute to the formation of the electron halo in the solar wind. However, the general origin of high bulk velocity electron beams in solar flares is poorly understood.

It is well known that solar flares accelerate electrons to a power-law energy distribution in the magnetic reconnection (MR) region. Theory and particle-in-cell simulations show that the power-law energetic electrons can be produced in the diffusion region of MR. However, the bulk velocity of the energetic electrons does not usually exceed the threshold of ETSI (larger than the local electron thermal speed) due to intense plasma heating and cannot trigger ETSI immediately and hence does not produce Type III radio bursts in the acceleration region. Many observations also found that the bulk velocity of energetic electrons reaches 0.1c-0.5c, which is about 3 to 10 times the local thermal speed as the energetic electrons continuously propagate upward for about 200 Mm away from the acceleration region, and Type III radio bursts are produced. However, it is still unclear what mechanism is responsible for such a high speed of energetic electrons.

Previous studies of beam formation in the solar corona focused on the maintenance of the beam after the triggering of Type III radio bursts. What effects govern electron beam formation before triggering Type III radio bursts remain unsolved. During propagation, electrons can experience three possible effects, i.e., Coulomb collisional scattering, background turbulence scattering, and magnetic focusing effects. The electron Coulomb collision rate in the inner corona is $\nu_e \sim 10^{-4}\ s^{-1}$ and the Coulomb heating timescale is about 10^4s. During this period, keV electrons (with a typical velocity about 1×10^3 km/s) travels 100 solar radii. Thus, the impact of Coulomb collisions on the transport of energetic electrons is negligible. The open magnetic field lines forming during MR decrease as they extend from corona to space. Since the magnetic fields change slowly in time and space compared to the time scale of electrons traveling in the corona, the magnetic moment of electrons is approximately conserved. Consequently, the conservation of electron magnetic momentum leads to an increased parallel velocity and a decreased perpendicular velocity, dubbed as magnetic focusing. However, the efficiency of magnetic focusing in forming a beam in the corona when scattering by background turbulence is included has not been investigated.

Using kinetic transport theory, we find, for the first time, that the bulk velocity of energetic electrons (electron beam) increases rapidly to a speed much higher than the local electron thermal velocity over a short distance of less than 0.35 solar radii (270 Mm). Using the observed velocity and location distributions of electron beam, our model shows that the temperature of flare acceleration regions ranges from 5 × 106K to 2 × 10^7K for beam velocities ranging from 0.1c to ~ 0.5c at locations > 200 Mm above the acceleration region. Our model also indicates that the acceleration region may have a boundary where the temperature decreases. As a result, the bulk velocity of beams can suddenly become more than three times (even up to 10 times) the coronal background thermal velocity and produce Type III radio bursts.

Description of the Model

The gyrophase averaged kinetic equation for the total electron distribution function has the form:

$$\frac{\partial f}{\partial t} + \mu v \frac{\partial f}{\partial r} + \frac{n_B}{2}\frac{(1-\mu^2)v}{r}\frac{\partial f}{\partial \mu} = \left(\frac{\delta f}{\delta t}\right)_{turb}. \qquad (1)$$

where (v, μ) is the magnitude of velocity and pitch-angle measured in the solar wind frame, r the heliocentric distance. $((\delta f/\delta t)_{turb}$ is the scattering term for whistler mode turbulence.

we approximate the open magnetic field of the solar flares as $B = B_0/r^{nB}$, where B_0 is the magnetic field at the inner boundary, then we have $d \ln B/dr = -n_B/r$, and the value of n_B comes in the transport equation while the exact value of magnetic field disappears.

$$\left(\frac{\delta f}{\delta t}\right)_{turb} = \frac{\partial}{\partial \mu}\left(D_{\mu\mu}\frac{\partial f}{\partial \mu}\right) + \frac{1}{v^2}\frac{\partial}{\partial v}\left(\frac{v^2}{m^2}D_{vv}\frac{\partial f}{\partial v}\right) + \frac{\partial}{\partial \mu}\left(\frac{1}{m}D_{\mu v}\frac{\partial f}{\partial v}\right) + \frac{1}{v^2}\frac{\partial}{\partial v}\left(\frac{v^2}{m}D_{v\mu}\frac{\partial f}{\partial \mu}\right),$$

$$D_{vv} = \frac{\Omega_e m^2 c^2 \pi}{3}\frac{A}{a}\left(\frac{\beta|\mu|}{a}\right)^{\frac{s-1}{3}};$$

$$D_{\mu v} = D_{v\mu} = -\frac{\Omega_e mc\pi}{3}\frac{A}{a}\left[\frac{\mu}{|\mu|}\left(\frac{\beta|\mu|}{a}\right)^{\frac{s-2}{3}} + \frac{\mu}{\beta}\left(\frac{\beta|\mu|}{a}\right)^{\frac{s-1}{3}}\right](1-\mu^2);$$

$$D_{\mu\mu} = \frac{\Omega_e \pi}{3}\frac{A}{a}\left[\left(\frac{\beta|\mu|}{a}\right)^{\frac{s-3}{3}} + \frac{2\mu}{\beta}\frac{\mu}{|\mu|}\left(\frac{\beta|\mu|}{a}\right)^{\frac{s-2}{3}} + \left(\frac{\mu}{\beta}\right)^2\left(\frac{\beta|\mu|}{a}\right)^{\frac{s-1}{3}}\right](1-\mu^2),$$

where $\beta = v/c$, $a = \Omega_e^2/\omega_{pe}^2$. A = 0.1 is normalization constant, and s = 2 the spectral index of whistler waves. To circumvent the difficulty in estimating accurately the intensity of whistler turbulence in the low corona, we assume a possibly unreasonably high level that is comparable to the strength of the mean magnetic field in the corona (i.e., $<\delta B^2>/B^2 \sim 1$, where $<\delta B^2>$ is the variance of the magnetic field fluctuations) with a power law spectrum with index −2. This is undoubtedly stronger turbulence than should realistically be expected (Tang et al. (2020)).

We first focus on the case with no scattering by turbulence ($(\delta f/\delta t)_{turb} = 0$), thereafter we add the scattering term and compare the two results.

The energetic electron VDF produced at the acceleration region of MR is used as the initialization at the inner boundary. A combination of a drifting Maxwellian (f_m) and a drifting power-law (f_p) is chosen to mimic the energetic electron VDFs with a drifting velocity U_d.

$$f(v, \mu \geq 0) = \delta f_m(v,\mu) + (1-\delta) f_p(v,\mu),$$

$$f_m(v,\mu) = n_0\left(\frac{m}{2\pi k_B T_{c0}}\right)^{3/2}\exp\left\{-\frac{m}{2k_B T_{c0}}\left[(v\mu - U_d)^2 + v^2(1-\mu^2)\right]\right\}$$

$$f_p(v,\mu) = n_0\frac{1}{4\pi}\frac{\alpha-3}{v_c^{3-\alpha}}\left\{\left[(v\mu - U_d)^2 + v^2(1-\mu^2)\right]^{1/2}\right\}^{-\alpha}$$

$$(v\mu - U_d)^2 + v^2(1-\mu^2) \geq v_c^2$$

where δ is the weight of Maxwellian, T_{c0} its temperature, n_0 the total electron number density at the inner boundary, v_c the critical velocity separating the power-law component from Maxwellian, and α the spectral indexes of the power-law.

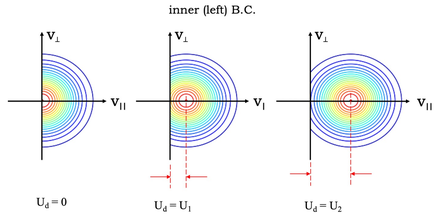

Figure 1. Example of different inner (left) boundary conditions with a drifting electron VDF.

We numerically solve the transport equation (1) to study the transport of electrons in the corona from 1.05 to 3.05 R_s to the center of the Sun. The critical velocity $v_c = 1.5v_{th0}$, where $v_{th0} = (2k_B T_{c0}/m)^{1/2}$ is the electron thermal velocity at the inner boundary. Adjust the parameters α and U_d to mimic the diverse power-law electron energy spectra and the drifts of electron outflows produced by MR acceleration, adjust n_B to mimic the open field lines in MR produced with different curvatures.

Numerical Results

We define the velocity of electron beam by integrating the VDF from v_{min}:

$$u_b = \frac{2\pi\int_{v_{min}(r,\mu)}^{\infty} dv \int_{\mu_{min}(r)}^{1} d\mu v^3 \mu f}{2\pi\int_{v_{min}(r,\mu)}^{\infty} dv \int_{\mu_{min}(r)}^{1} d\mu v^2 f}$$

where $\mu_{min}(r)$ is the cosine of the maximum pitch-angle of electron VDF at distance r. The radial evolution of u_b are plotted in A1 and A2.

The growth rate of electron beam velocity as $\chi_u = (u_b - u_{b0})/u_{b0}$ where u_{b0} is the initial u_b at the inner boundary. The radial evolution of χ_u are in A3 and A4.

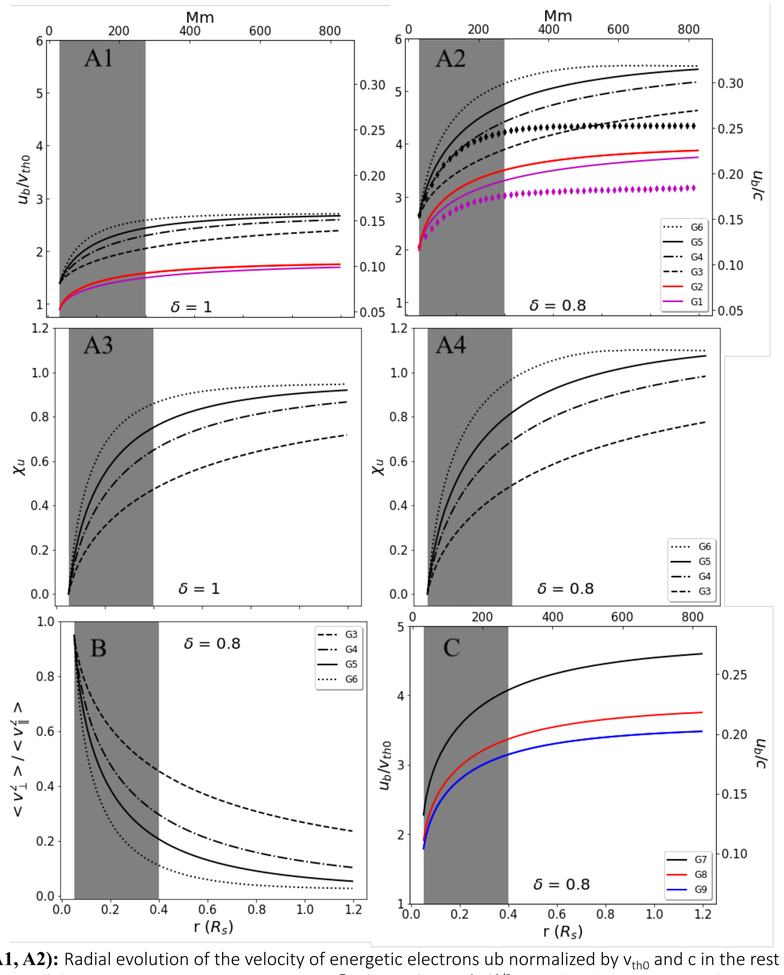

(A1, A2): Radial evolution of the velocity of energetic electrons ub normalized by v_{th0} and c in the rest frame of the Sun using a temperature $T_{c0} = 10^7$ K ($v_{th0} = (kBTc0/m)^{1/2}$. A1: The electron VDF at the inner boundary is a Maxwellian only (δ = 1). A2: The electron VDF at the inner boundary is a combination of a Maxwellian with weight δ = 0.8 and an isotropic power-law with α = 4 and weight 0.2. Black and magenta diamonds show the results of cases of α = 4, U_d = 0, n_B = 2 and α = 4, $U_d = v_{th0}$, n_B = 3 respectively under the effect of maximum resonant wave-particle interactions..

(A3, A4): Radial evolution of electron beam velocity growth rate χ_u.

B: Radial evolution of kinetic energy ratio of electron beam.

C: Radial revolution of u_b with different power-law indexes α = 4, 6 and 8.

Figure 3 A1 and A2 present the radial evolution of the bulk velocity in the rest frame of the Sun for twelve cases. u_b under all conditions increases sharply from the inner boundary 0.05 to 0.4 Rs (i.e., over 0.35 Rs, or 270 Mm), indicating that magnetic focusing increases the parallel bulk velocity when energetic electrons move upward along magnetic field lines. Compared with A1, A2 shows that the energetic electrons with a power-law energy spectrum escaping from the acceleration region can reach a higher bulk velocity, which is about three times larger than the thermal velocity vth0. The decreasing electron temperature with distance in the corona leads to a decrease of the local electron thermal velocity ($v_{th0} > v_{th}$). Therefore, above 0.35 Rs (270 Mm), energetic electrons likely have a bulk velocity u_b that is a much larger value than the local electron thermal velocity, i.e., $u_b \gg v_{th}$. Energetic electrons with a larger bulk velocity can trigger a stronger ETSI and produce Type III radio bursts, which is consistent with the observations that type III radio bursts are always found above a certain distance (> 100 Mm) from the acceleration region.

Magnetic focusing can increase the electron bulk velocity much more rapidly if more energetic electrons with a power-law tail are present, thus triggering ETSI and producing type III radio bursts. Second, the n_B in magnetic field $B = B_0/r^{nB}$ also affects the radial evolution of u_b and its percentage increase χu. As n_B increases from n_B = 1 to 3, and to 5, both the electron bulk velocity u_b and its percentage increase χu increase faster and reaches a larger value. Consequently, in a more rapidly decreasing magnetic field, we expect more Type III radio bursts to occur at distances closer to the acceleration region of MR.

Discussion and Conclusion

Magnetic focusing caused by a magnetic field rapidly decreasing with solar radial distance can increase the bulk velocity of energetic electrons over less than 0.35 solar radii (270 Mm) to be much larger than the local electron thermal velocity. Theoretical studies and simulations have shown that energetic electrons with bulk velocity much larger than the local thermal speed ($u_b \gg v_{th}$) can trigger a strong ETSI and produce Type III radio bursts, which is consistent with the observations that type III radio bursts are always found above a certain distance (> 100 Mm) from the acceleration region. Moreover, the bulk velocity of energetic electrons reaches as high as 0.2c, which is also consistent with the observed typical electron beam velocity range of 0.1c ~ 0.5c in a solar flare. This is consistent with observations that the electron beams that produce type III radio bursts are usually found above 100 Mm above the photosphere. In the case of energetic electrons with a harder power-law energy spectrum (smaller α), the electron beams achieves a higher velocity, indicating that the Type III radio bursts starting location may depend on the energetic electron spectral index. Energetic electrons with higher bulk velocity can trigger the ETSI and produce type III radio bursts at a location closer to the acceleration region.

By comparing with observed electron beam velocities, we can estimate the coronal plasma environment of type III radio bursts. In Figure 3, red dots show the radial distribution of observed electron beam velocities for type III bursts given by Reid & Kontar (2018). Theoretically, the electron beam velocities are calculated using two different initial temperatures T_{c0} (2×10^7 K and 5×10^6 K) in acceleration region. The radial evolution of the velocities normalized by the electron thermal velocity in the coronal background ($u_b/v_{the,cb}$) and acceleration region (u_b/v_{th0}) are plotted. Type III radio bursts are observed at a distance beyond 0.6 Rs, which is above the region where the electron beam velocity increases sharply (from 0.05 to 0.4 Rs). The electron beam velocities do not increase much thereafter and tend to plateau in this region. In considering the range of the observed (red dots) beam speeds and noting that the theoretical beam speeds bracket this range, Figure 3 suggests that the temperature in the acceleration region ranges from $5 \times 10^6 \sim 2 \times 10^7$ K, which is consistent with observations (Benz (2017)). Figure 3 suggests that the velocity of electron beams that produce Type III radio bursts, in general, is 3 times larger than the corona electron velocity with $T = 10^6$ K, and some even can reach up to 10 $v_{the,cb}$. From the observations and our model, we can infer that the acceleration region and the background plasma have a distinct boundary where the temperature has a sharp decrease. This can explain why some beam velocities can reach speeds up to 10 $v_{the,cb}$ which is much larger than the theoretical threshold to trigger ETSI (3 v_{th0}). Such high velocity electron beam can trigger a strong ETSI, generate long-lived type III radio bursts, consistent with theory.

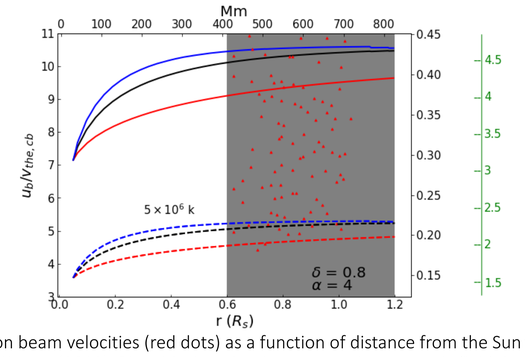

Figure 3. Electron beam velocities (red dots) as a function of distance from the Sun for type III bursts given by Reid & Kontar (2018). Blue, black and red represent the magnetic field decrease as r^{-5}, r^{-3} and r^{-1}. The temperatures of the coronal background and the acceleration region are 106 K and 107 K, respectively. Calculated bulk velocities are normalized by electron thermal velocity of the corona background ($u_b/v_{the,cb}$) and acceleration region (u_b/v_{th0}). The shaded area indicates the distance beyond 0.6 Rs (about 400 Mm) where type III radio bursts are always being observed.

This work is supported by NASA HSR program No. 80NSSC21K0031, Heliophysics Career award No. 80NSSC19K1106, NSF CAREER 2144324, and an NSF EPSCoR RII-Track-1 Cooperative Agreement OIA-1655280.